Research on Recurrent Neural Network Based Crack Opening Prediction of Concrete Dam

Jin Wang[1,2], Yongsong Zou[2], Peng Lei[2], R. Simon Sherratt[3], Lei Wang[4]

[1] School of Computer & Communication Engineering, Changsha University of Science & Technology, China
[2] School of Hydraulic Engineering, Changsha University of Science & Technology, China
[3] Department of Biomedical Engineering, the University of Reading, U.K.
[4] School of Civil Engineering, Changsha University of Science & Technology, China
jinwang@csust.edu.cn, zougenshen@126.com, dolaimy@163.com,
r.s.sherratt@reading.ac.uk, leiwang@csust.edu.cn

Abstract

The concrete dam can prevent flooding events and generate a vast amount of electricity, and it is a critical national infrastructure. However, it is easy to get cracked, and cracks usually pose significant potential threats to the safety of the concrete dam. Many researchers have done much research on dam crack protection and explored various rules to protect the concrete dam from cracks. However, the complex and irregular distribution of cracks make this task a very challenging research issue. In this paper, the feature importance of crack influencing factors is firstly analyzed. Then, the Recurrent Neural Network (RNN) is introduced for dam crack modeling. Next, the crack width of the Longyangxia Dam is modeled and tested by using the Gated Recurrent Unit (GRU) and Long Short-Term Memory (LSTM). Finally, experimental results show that our proposed RNN-based method can effectively predict the crack change of the concrete dam.

Keywords: Concrete dam, Crack opening prediction, LSTM, Recurrent Neural Network

1 Introduction

Neural network algorithms can automatically learn the characteristic information of complex systems [1-2], and their main advantages are that they can learn uncertain and sophisticated systems. Thus, neural network algorithms are widely used, such as machine vision [3-4], internet of vehicles [5], wind power [6], water conservancy [7-9], wireless sensor networks (WSNs) [10-12]. Recurrent Neural Network (RNN) is a kind of neural network that can solve the temporal problems effectively [13-14]. This paper focuses on the modeling of concrete dam crack with RNN.

The concrete dam can prevent flooding events and generate a vast amount of electricity, and it is a critical national infrastructure. However, dames are prone to get cracked in practical projects. Cracks pose a severe threat to the safety of concrete dam structure, and about a third of dam failures are caused by cracks [15-16]. To prevent damage to the reservoir caused by cracks, many researchers have carried out a lot of experimental studies on dam cracks, such as dam crack path [17]and dam crack criteria: stress pattern [18], energy pattern [19], stress intensity factor [20-21] criterion.

The cracks are caused by the external force. The difference between the stress intensity factor and the cohesive intensity factor at the crack tip produces the crack. The reason for Gongboxia Dam crack by structural stress and temperature stress is analyzed in [22], where temperature stress is the main factor. And the water level of the reservoir may be the leading cause of the vertical crack. Authors in [23] analyzed the main reason of Xiaowan Dam cracks. The change of dam stress and the deformation of the dam body result in the instability of dam structure, which leads to cracks. In [24], the scaled boundary finite element method coupled with the cohesive crack model was extended to investigate the hydraulic fracture at the dam-foundation interface. The water pressure in fracture was studied therein. The results showed that the water pressure of the crack would cause the overflow to increase and the crack to expand.

The prediction of crack opening, crack length and crack direction of concrete surface are of great significance for improving the service life and sustainability of structures. In the paper [25], the propagation criterion of I-II mixed mode crack in concrete is presented. The criterion combined with the finite element method can predict the initial crack load, ultimate bearing capacity and crack development trajectory of mixed-mode I–II fracture in concrete structures accurately. The paper [26] can predict the propagation path of the crack by characterizing the

*Corresponding Author: Lei Wang; E-mail: leiwang@csust.edu.cn
DOI: 10.3966/160792642020072104024

fracture characteristics of spatial variation as random fields, simulated the propagation of the heterogeneous cohesive crack. Paper [27] proposed a judgment method of crack generation. It can predict the crack propagation. However, these methods require highly accurate boundary conditions for numerical simulation [28].

In order to explore reliable fracture models, this paper introduced the RNN to train the model. We aim to train the RNN model, which can predict the crack opening in the next 11 months based on the historical data of 10 months data. Training a neural network requires many data. The internet of things can provide data by WSNs [29-33]. This paper, the training data comes from the sensors of the Longyangxia Dam. The paper [34-35] showed the novel calculation method of vector spaces. It is enlightening for us to propose a new linear similarity evaluation method.

The main contributions of this paper are summarized as follows: 1) The RNN is applied to study the concrete dam cracks problem. The crack of Chinese Longyangxia Dam is analyzed and modeled, and the validity of the model is verified. 2) The loss function of RNN training is defined to increase the accuracy of the training process. 3) We proposed a method to evaluate the accuracy of linear regression prediction problems.

2 Background

2.1 Recurrent Neural Network

Many improved RNNs have emerged in recent years. LSTM and GRU are famous for their excellent performance in the temporal problems. The authors in [36] proposed the Long short-term memory (LSTM) to improve the RNN. It introduced the concept of gate. The LSTM cell has an input gate, an output gate, and a forget gate. The input gate is used to pick useful information. The forget gate is used to delete useless information. The output gate is used to control output information. Formula 1-7 is LSTM.

$$f^t = sig \bmod(W_f[h^{t-1}, x^t] + b_f) \quad \textbf{(1)}$$

$$i^t = sig \bmod(W_i[h^{t-1}, x^t] + b_i) \quad \textbf{(2)}$$

$$g^t = \tanh(W_g[h^{t-1}, x^t] + b_g) \quad \textbf{(3)}$$

$$z^t = sig \bmod(W_z[h^{t-1}, x^t] + b_z) \quad \textbf{(4)}$$

$$c^t = i^t g^t + f^t c^{t-1} \quad \textbf{(5)}$$

$$h^t = z^t \tanh(c^t) \quad \textbf{(6)}$$

$$O^t = soft \max(W_0 h^t + b_0) \quad \textbf{(7)}$$

where t is the time. f^t, i^t, z^t are the forget gate, input gate, and output gate, respectively. x^t is the input matrix. h^t is the hidden output at time t. h^{t-1} is the hidden output at time t-1 which used to store short-term information. O^t is the output. c^t is used to save long term information. W_f, W_i, W_g, W_z, W_o are the weight parameter matrix of the corresponding function. b_f, b_i, b_g, b_z, b_o are the bias of the corresponding function.

Due to the gate scheme, LSTM can capture long-term dependencies. Nevertheless, the LSTM cell is too complicated. There are too many training parameters, which need more computing resources. On the one hand, researching the scheme of high-performance computing, such as edge computing [37-41]. On the other hand, authors [42] simplified the structure of the LSTM cell, proposed the GRU. It simplified the input gate, renamed it to update gate, and removed the output gate. The structure of the GRU cell is more straightforward than that of the LSTM cell, which reduced the training parameters. The equations are list below in (8)-(12).

$$z^t = sig \bmod(W_z x^t + R_z h^{t-1} + b_g) \quad \textbf{(8)}$$

$$r^t = sig \bmod(W_r x^t + R_r h^{t-1} + b_r) \quad \textbf{(9)}$$

$$\tilde{h}^t = \tanh(W x^t + R(r^t * h^{t-1})) \quad \textbf{(10)}$$

$$h^t = (1 - z^t) h^{t-1} + z^t \tilde{h}^t \quad \textbf{(11)}$$

$$O^t = soft \max(W_0 h^t + b_0) \quad \textbf{(12)}$$

where * is Hadamard product. t is the time. x^t is the input matrix at time t. h^t is the hidden output at time t. h^{t-1} is the hidden output at time t-1. It's used to store short-term memory information. z^t is the update gate. r^t is the reset gate. W_z, W_r, W, W_o are the weight parameter matrix of the corresponding function. b_z, b_r, b_o are the bias of the corresponding function. Although the GRU simplifies the LSTM parameters, the performance is almost similar.

On the other hand, the time flow of LSTM and GRU is one-way in the training process. LSTM and GRU only use historical information to train a model. However, we need to use temporal information to train the current state sometimes. Therefore, the paper [43] proposed the Bidirectional RNN (BiRNN), which can be trained by using historical information or future information.

2.2 Longyangxia Dam

Longyangxia hydropower station is an arch dam in

the upper reaches of the Yellow River in China. Its main parts include the main dam, the gravity piers, the gravity auxiliary dam, the concrete arch dam, the drainage buildings, the diversion buildings, and the hydropower station (see Figure 1). The total length of the water-retaining front of the Longyangxia Dam is 1226m. And the length of the main dam is 396m. The check flood level of the reservoir is 2607m. The average water level in front of the dam is 2600m. The flood season limit water level is 2594m. The Longyangxia project began in December 1979, and the water storage began in October 1986. After water storage, cracks began to appear. By 1999, about 135 cracks appeared on the downstream surface at the elevation of 2500 ~ 2570m. And 125 cracks were monitored by using sensors such as crack gauge and thermometer sensors. The recorded data of crack included crack width and crack temperature. The recorded data of the environment included upstream water level, downstream water level, and environmental temperature.

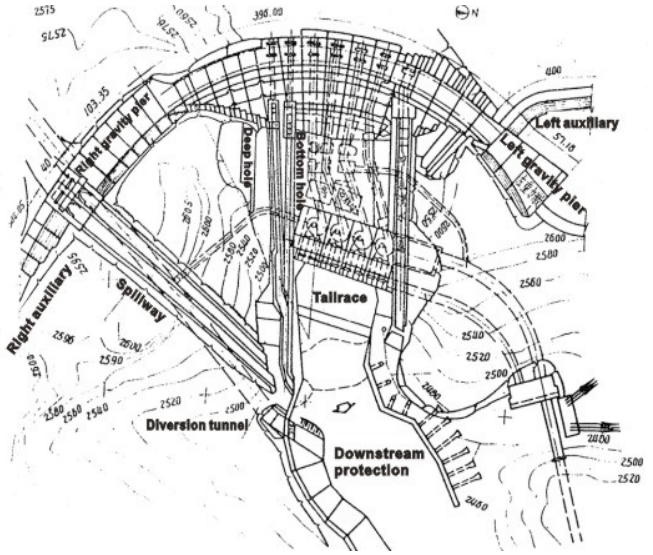

Figure 1. General layout plan of Longyangxia Dam

2.3 Crack Opening

When the crack tip reaches the maximum allowable strain, the crack will continue to expand. The calculation formula of the crack opening is shown in Equation 13.

$$K_0 = \frac{4\sigma}{e}\sqrt{(a + r_p^*) - x} \tag{13}$$

where K_0 is the crack width, E is the elastic modulus, σ is the stress around the crack, a is half of the crack length, r_p^* is the radius of the plastic zone, and x is the distance from the crack tip to the point. The crack opening is proportional to the stress, which is caused by the external load.

3 Dam Crack Opening Prediction Model

3.1 Network Structure

LSTM and GRU have an excellent performance in sequence data [44-45]. In this paper, the networks with recurrence depth of 4 are studied (Figure 2). The input layer and hidden layers are recurrent layers. The output layer is Dense. To compare different recurrent framework of RNN, we employ three scheme. It is shown in Table 1. Scheme A consists of GRU and LSTM. The input layer is GRU. The remaining recurrent layers are LSTM, LSTM, and GRU, respectively. Scheme B consists of LSTM. The recurrent layers are LSTM. Scheme C consists of GRU. The recurrent layers are GRU.

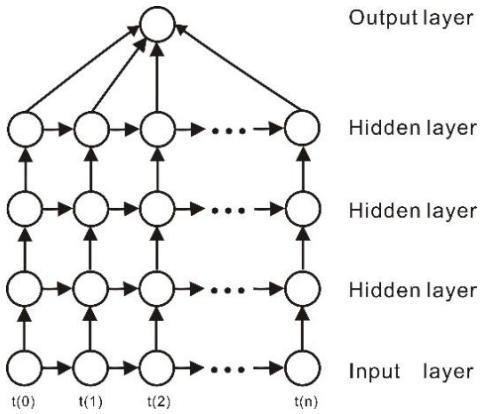

Figure 2. Network structure. t(n) is the input at time n

Table 1. RNN configuration

Layers	Scheme A	Scheme B	Scheme C
1	GRU	LSTM	GRU
2	LSTM	LSTM	GRU
3	LSTM	LSTM	GRU
4	GRU	LSTM	GRU
5	Dense	Dense	Dense

3.2 Improved Loss Function

Mean Absolute Error (MAE) and Mean Square Error (MSE) are commonly used loss functions in regression problems. MAE is shown in Equation (14). MSE is shown in Equation (15).

$$MAE = \frac{\sum_{i=1}^{n} | y_i - y_i^p |}{n} \tag{14}$$

$$MSE = \frac{\sum_{i=1}^{n} | y_i - y_i^p |^2}{n} \tag{15}$$

where y_i is the real value, y_i^p is the predicted value, and n is the length of training.

For better robustness, we combine the equation 14 and 15. And we defined a loss function, Mean Absolute and Square Error (MASE) in Equation 16 below.

$$MASE = \alpha * MAE + (1-\alpha) * MSE \quad \textbf{(16)}$$

where a is the weight coefficient. When training the model, the value of α needs to be adjusted according to the training loss and validate loss.

3.3 Experimental Setup

In this paper, the cracks data of Longyangxia Dam were used to train the model. The researchers have measured 125 of the 135 cracks from the year 1985 to 2000.

3.3.1 Data Filtering

Some cracks cannot be used for training due to a few training samples. Therefore, we deleted the crack that training samples less than 40. Since recording frequency was different, sometimes once a month, sometimes several times a month. Only one set of valid values was retained each month to align the data. The useless values were replaced by an average of the first five times.

- There are some defects in the data of cracks.
- There are a few cracks that did not measure enough data.
- There are missing values and useless values.
- The recording frequency of each crack is not fixed.

3.3.2 Standardization

The basis of the objective function is that assuming all of the features are zero means and have the same magnitude of variance in most learning algorithms. If the variance of a feature is several magnitudes more significant than that of others, it will occupy a dominant role in the learning algorithm in the training process. Other features cannot be adequately learned. It results in the low accuracy of the trained model.

In Figure 3, there are some outliers in the raw data (blue line). The outliers will harm the convergence of the network. The outliers need to be removed from the raw data to improve the accuracy of RNN. In this paper, the Tukey algorithm was used to remove outliers. First, calculating the quarter digit (Q_1) and three-quarters digit (Q_3) of the data array. Secondly, calculating the quartile space ($I = Q_3 - Q_1$). Finally, the value less than $Q_1 - 1.5 * I$ or greater than $Q_3 + 1.5 * I$ is regarded as outliers. The blue line is the raw data of D11J41 crack, and the red line is the result of Tukey in Figure 3. It shows that the Tukey algorithm can remove outliers effectively.

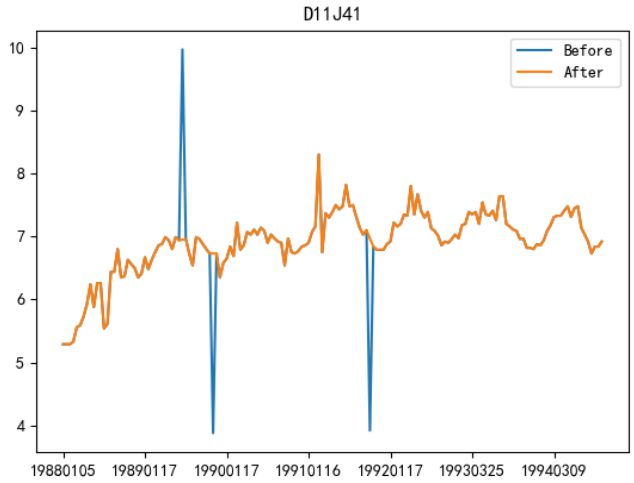

Figure 3. Results of the Tukey algorithm. The blue line is the raw data of D11J41

After data filtering and standardization, we retained the data. Then, we divided data into three groups with 80 training sets (6935 samples), six valid sets (595 samples), and 3 test sets (169 samples), as is shown in Table 2.

Table 2. Data sets

Train samples	Validate samples	Test samples
7130	620	169

3.3.3 Impact Factor Analysis

From equation 13, it can be seen that the crack opening is related to the surrounding stress. But for the concrete dam, what are the factors related to the stress? We use the tree integration model XGBoost [46] algorithm to evaluate six measurement factors, upstream water level, downstream water level, crack temperature, environment temperature, upstream, and downstream water level difference, environment and crack temperature difference.

Table 3 shows evaluation results where Crack-temp is the accompanying temperature of the crack. Up-stream is the water level upstream of the reservoir. Down-stream is the water level downstream of the reservoir. Env-temp is the ambient temperature. Water-diff is the difference between the water level upstream and downstream. Temp-diff is the difference between ambient temperature and crack temperature.

Table 3. The feature importance of the crack opening

Feature	Crack-temp	Upstream	Downstream	Env-temp	Water-diff	Temp-diff
Influence	35.57%	17.99%	11.69%	10.71%	12.25%	11.79%

It can be seen that all the six features have an impact on the change of crack opening. The impact of Crack-temp is the largest (35.57%). The second is the Upstream, 17.99%. Next is the Water-diff,12.25%. Then, the Temp-diff is 11.79%.

3.4 Metrics

The prediction of concrete cracks is a linear regression problem. The prediction accuracy of the linear regression problem can be determined from two aspects.

(1) Whether the shape is the same, that is, the linear correlation between the predicted value and the real value.

(2) Whether the two curves overlap.

Firstly, we use the Pearson correlation coefficient to evaluate the predicted results. Then, we proposed the Overlap Rate (OR) to evaluate the overlap.

3.4.1 Pearson Correlation Coefficient

Pearson correlation coefficient formula (17-18).

$$\rho_{r,p} = \frac{\mathrm{cov}(R, P)}{\sigma_r \sigma_p} = \frac{E((R-\mu_r)(P-\mu_p))}{\sigma_r \sigma_p} \tag{17}$$

$$\rho_{r,p} = \frac{\Sigma RP - \frac{\Sigma R \Sigma P}{N}}{\sqrt{(\Sigma R^2 - \frac{(\Sigma R)^2}{m})(\Sigma P^2 - \frac{(\Sigma R)^2}{m})}} \tag{18}$$

where R is the array of real values. P is the array of predicted values. M is the array length. R is the array of actual values. P is the array of predicted values. Pearson coefficient is defined as: "*The covariance cov(R, P) between array R and array P divided by the product of their respective standard deviations* $\sigma_r \sigma_p$ *is the Pearson correlation coefficient* $\rho_{r,p}$ *between array R and array P*". $\rho_{r,p} \in [0,1]$, $\rho_{r,p} = 0$ means there is no correlation between the two arrays.

3.4.2 Overlap Rate

According to the linear regression characteristics, we proposed the OR of the real curve and the predicted curve. We set the objective function of the linear regression problem as formula 19.

$$y_t = f(x_t) \tag{19}$$

where $t = t_0, t_1, t_2, \ldots\ldots t_{m-1}$ is the time. x_t is the input feature array at the time t. y_t is the output array at the time t. We defined the OR as: "*If the predicted curve is positively correlated with the real curve, in* $t \in [t_0, t_{m-1}]$, *the predicted function integral minus the true function integral, and then we divide by the absolute value of the true function integral*".

It is shown in formula 22 below.

$$\delta_{r,p} = 1 - \frac{|\int_{t_0}^{t_{m-1}} y^P \, dt - \int_{t_0}^{t_{m-1}} y^R \, dt|}{|\int_{t_{a-1}}^{t_a} y \, dt|} \tag{20}$$

$$\int_{t_{a-1}}^{t_a} y \, dt = \frac{|(y_{t_a} + y_{t_{a+1}})|}{2} \tag{21}$$

where m is the number of continuous predictions. $\alpha \in [0, m-1]$. $\delta_{r,p}$ can be calculated as

$$\delta_{r,p} = 1 - \sum_{n=1}^{m-1} \frac{|(y_{t_n}^P + y_{t_{n-1}}^P| - |(y_{t_n}^R + y_{t_n-1}^R)|)|}{|y_{t_n}^R + y_{t_n-1}^R|} \tag{22}$$

where y^R is the real value at time t. y^P is the predicted value at the time t. m is the sequence length. $\delta_{r,p} \in [0,1]$, if $\delta_{r,p} = 1$. $\delta_{r,p} = 0$ when there is no overlap between two curves.

Hence, in this paper, Pearson's correlation between the predicted value and real value was used to evaluate the linear correlation. The $\delta_{r,p}$ was used to evaluate the agreement between the predicted curve and the actual curve. Therefore, the definition of Linear Regression Accuracy (LRA) we proposed is shown as

$$\gamma_{r,p} = \beta \delta_{r,p} + (1-\beta)\rho_{r,p} \tag{23}$$

where $r_{r,p}[0,1], r_{r,p} = 0$ means prediction accuracy is 0. $r_{r,p} = 1$ means the prediction accuracy is 100%. $\beta \in [0,1]$ is the weight coefficient. $\delta_{r,p}$ is the overlap rate, which is used to represents the overlap area of the two curves. $\rho_{r,p}$ is the Pearson correlation coefficient, which is used to quantify the morphological similarity of two curves. β can be set according to the actual situation. In this paper, β is set to 0.5.

4 Experimental Results

4.1 Model Training

The inputs of RNN is a 3-dimensional (N, W, F) array, where N is the number of training sequences, W is the length of the sequence, and F is the number of features of each sequence. According to the conclusion of section 3.2.4, we selected the input features: historical crack opening, crack temperature, upstream water level, temperature difference, and water level difference. So, the number of input features is 5. The output is the crack opening. Therefore, the dimension of the output data is 1. Our goal is to use the historical data from the first ten months to predict the crack opening in the 11th month, So the sequence length (window size) is 10. The input array of our model is (N,10,5).

Then, We used the training sets to train three models of crack opening with the three schemes. Figure 4 records the curve of the train and the validate loss of scheme A in the training process. It can be seen from the figure that with the decrease of the error, the validate loss became smaller and smaller. With the increase of epoch, the validate loss is stable at about 0.02. It shows that the trained model can meet the requirements.

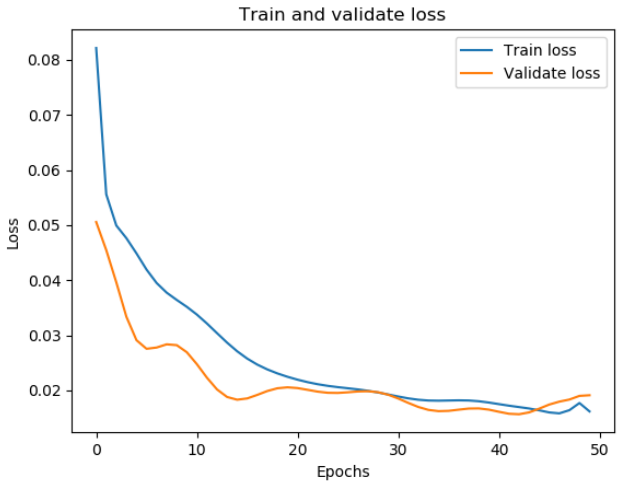

Figure 4. The loss function of scheme A curve during training

4.2 Results Analysis

Crack D11J41, D11J42, and D11J52 are the test data sets. The crack opening of test data sets is predicted by using the trained model. The precision of each crack is calculated according to formula 22. Table 4 shows the test results of scheme A. Table 5 shows the test results of scheme B. Table 6 shows the test results of scheme C.

Table 4. The test results of scheme A

Crack	Overlap (%)	Pearson (%)	Accuracy (%)
D11J41	98.57	99.22	98.89
D11J42	89.79	91.92	90.85
D11J51	96.35	98.75	97.55
Average	94.90	96.63	95.76

Table 5. The test results of scheme B

Crack	Overlap (%)	Pearson (%)	Accuracy (%)
D11J41	89.04	99.09	94.07
D11J42	89.21	93.81	91.51
D11J51	96.35	99.21	94.91
Average	91.52	97.37	93.64

Table 6. The test results of scheme C

Crack	Overlap (%)	Pearson (%)	Accuracy (%)
D11J41	89.77	99.23	94.50
D11J42	89.63	95.68	92.65
D11J51	88.66	98.94	93.80
Average	89.35	97.95	93.65

From Table 4 to Table 6, we can know that the highest accuracy is scheme A. And, the precision of scheme A is about the same as that of scheme B. It shows that the composite structure of LSTM and GRU can play better performance of RNN in the model of dam crack. Figure 5 to Figure 7 show the results of scheme A. The figures show that the predictive curve is good agreement with the real curve. The figures also confirm the results of Table 4. It shows that the LRA can evaluate the regression accuracy effectively.

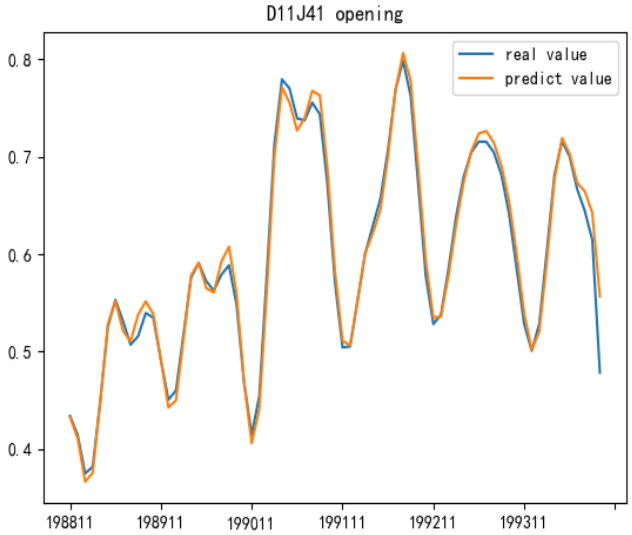

Figure 5. D11J41 predicted the results of scheme A

The raw data of crack D11J41 began in September 1986 and ended with 186 times in December 1994. After data alignment, only one set of valid values was retained every month. So, 82 months of data from January 1988 to December 1994 were retained for training. During the test, the crack opening of the back 72 months was predicted. Figure 5 shows the predicted results of crack D11J41. From Figure 5, It can be seen from the results that there is a highly linear correlation between the predicted curve and the real curve. According to table 4, the prediction LRA is 98.89%. The Pearson coefficient is 99.22%. The OR is 98.57%. The results indicated that the predicted curve is the same as the actual curve exactly.

The raw data of crack D11J42 began in September 1986 and ended with 122 times in March 1992. After data alignment, only one set of valid values is retained each month, so 51 sets of data are used for actual training. During the test, the crack width over the next 41 months was predicted. Figure 6 shows the predicted results of crack D11J42. It can be seen that the predicted curve is almost the same as the actual curve. According to table 4, the prediction LRA is 90.85%. The OR is 89.79%. The Pearson coefficient is 91.92%.

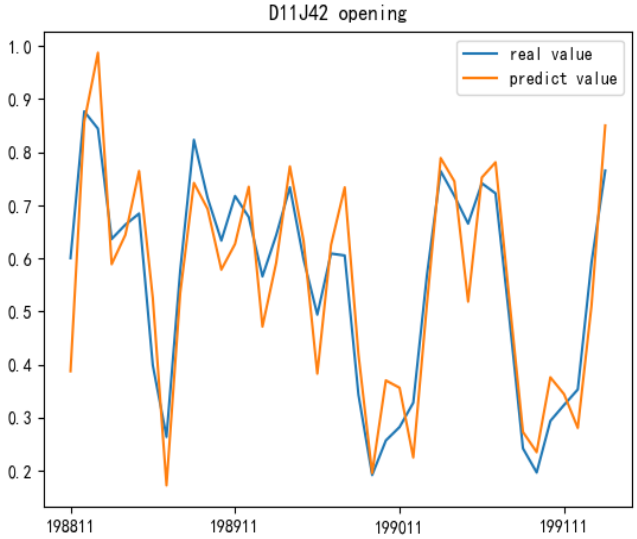

Figure 6. D11J42 predicted results of scheme A

The actual recorded data of crack D11J51 began in January 1988 and ended with 132 times in June 1993. After data alignment, 66 months of data were retained for training. During the test, the crack opening of the back 56 months was predicted. Figure 7 shows the comparison between the real value and the predicted value of crack D11J51, where the real value of the blue line and the predicted value are shown in orange. The predicted curve and the real curve is correlated highly. According to table 4, the prediction LRA is 97.55%. The Pearson coefficient is 98.75%. The OR is 96.35%.

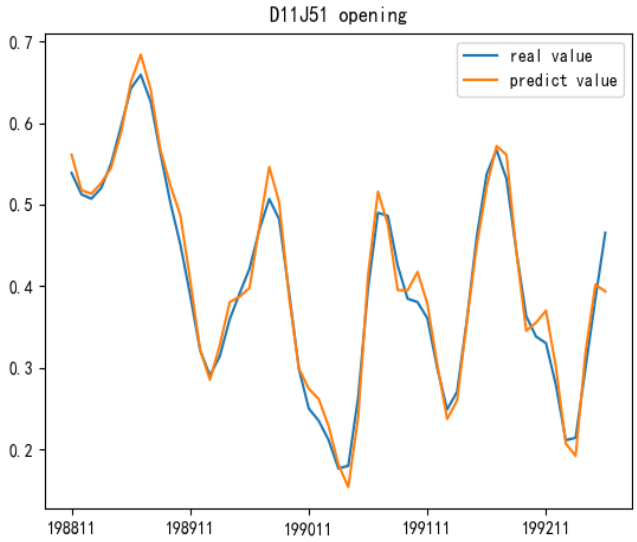

Figure 7. D11J51 predicted results of scheme A

5 Conclusion

This paper introduced RNN to train the model of the dam crack in the field of hydraulic engineering. We trained a crack opening model of the concrete dam with the crack data of Longyangxia Dam, and predict the crack opening of the 11th month with the historical data of 10 months. XGBoost algorithm was used to analyze the feature importance of crack influencing factors. The results showed that the four factors influence crack opening: crack temperature, upstream water level, the difference between upstream and downstream water level, and the difference between environment and crack temperature. Next, we proposed LRA to evaluate the accuracy of the linear regression problem. The LRA can evaluate the regression accuracy effectively. Then, the Longyangxia Dam crack data were used to train the crack model. Finally, the LRA was used to evaluate the model test results. The experimental results proved the effectiveness of RNN in dam crack modeling.

Acknowledgments

This work is supported by the National Natural Science Foundation of China (61772454). This work is funded by National Key Research and Development Program of China (2019YFC1511000).

References

[1] R. Socher, B. Huval, C. D. Manning, A. Y. Ng, Semantic Compositionality Through Recursive Matrix-vector Spaces, *2012 Joint Conference on Empirical Methods in Natural Language Processing and Computational Natural Language Learning*, Jeju Island, Korea, 2012, pp. 1201-1211.

[2] D. Zeng, K. Liu, S. Lai, G. Zhou, J. Zhao, Relation Classification via Convolutional Deep Neural Network, *25th International Conference on Computational Linguistics*, Dublin, Ireland, 2014, pp. 2335-2344.

[3] Y. Chen, W. Xu, J. Zuo, K. Yang, The Fire Recognition Algorithm Using Dynamic Feature Fusion and IV-SVM Classifier, *Cluster Computing*, Vol. 22, No. 3, pp. 7665-7675, May, 2019.

[4] J. Donahue, L. A. Hendricks, S. Guadarrama, M. Rohrbach, S. Venugopalan, K. Saenko, T. Darrell, Long-term Recurrent Convolutional Networks for Visual Recognition and Description, *IEEE Conference on Computer Vision & Pattern Recognition*, 2015, Boston, United States, pp. 2625-2634.

[5] T. Wang, Z. Cao, S. Wang, J. Wang, L. Qi, A. Liu, M. Xie, X. Li, Privacy-enhanced Data Collection Based on Deep Learning for Internet of Vehicles, *IEEE Transactions on Industrial Informatics*, pp. 1-1, December, 2019.

[6] J. Pan, P. Hu, S. Chu, Novel Parallel Heterogeneous Meta-Heuristic and Its Communication Strategies for the Prediction of Wind Power, *Processes*, Vol. 7, No. 11, p. 845, November, 2019.

[7] M. De Granrut, A. Simon, D. Dias, Artificial Neural Networks for the Interpretation of Piezometric Levels at the Rock-Concrete Interface of Arch Dams, *Engineering Structures*, Vol. 178, pp. 616-634, January, 2019.

[8] H. Hwang, J. Oh, K. Lee, J. Cha, E. Choi, Y. Yoon, J. Hwang, Synergistic Approach to Quantifying Information on a Crack-based Network in Loess/Water Material Composites Using

Deep Learning and Network Science, *Computational Materials Science*, Vol. 166, pp. 240-250, August, 2019.

[9] G. Bayar, T. Bilir, A Novel Study for the Estimation of Crack Propagation in Concrete Using Machine Learning Algorithms, *Construction & Building Materials*, Vol. 215, pp. 670-685, August, 2019.

[10] J. Wang, Y. Gao, W. Liu, A.K. Sangaiah, H. Kim, An Intelligent Data Gathering Schema with Data Fusion Supported for Mobile Sink in Wireless Sensor Networks, *International Journal of Distributed Sensor Networks*, Vol. 15, No. 3, p. 1550147719839581, March, 2019.

[11] Y. Chen, J. Tao, Q. Zhang, K. Yang, X. Chen, J. Xiong, R. Xia, J. Xie, Saliency Detection via the Improved Hierarchical Principal Component Analysis Method, *Wireless Communications & Mobile Computing*, Vol. 2020, pp. 1-12, May, 2020.

[12] J. Wang, Y. Gao, C. Zhou, R. S. Sherratt, L. Wang, Optimal Coverage Multi-path Scheduling Scheme with Multiple Mobile Sinks for WSNs, *CMC-Computers Materials & Continua*, Vol. 62, No. 2, pp. 695-711, March, 2020.

[13] Y. Yu, X. Si, C. Hu, J. Zhang, A Review of Recurrent Neural Networks: LSTM Cells and Network Architectures, *Neural Computation*, Vol. 31, No. 7, pp. 1235-1270, July, 2019.

[14] R. Jozefowicz, W. Zaremba, I. Sutskever, An Empirical Exploration of Recurrent Network Architectures, *32nd International conference on machine learning*, Lille, France, 2015, pp. 2342-2350.

[15] J. C. Kishen, K. D. Singh, Stress Intensity Factors Based Fracture Criteria for Kinking and Branching of Interface Crack: Application to Dams, *Engineering Fracture Mechanics*, Vol. 68, No. 2, pp. 201-219, February, 2001.

[16] J. Chai, S. Li, Analysis of Seepage Through Dam Foundation with Closed System of Grouting Curtain, Drainage and Pumping Measures, *4th International Conference on Dam Engineering*, Nanjing, China, 2004, p. 171-176.

[17] S. Zhang, G. Wang, X. Yu, Seismic Cracking Analysis of Concrete Gravity Dams with Initial Cracks Using the Extended Finite Element Method, *Engineering Structures*, Vol. 56, pp. 528-543, November, 2013.

[18] J. Červenka, J. C. Kishen, V. E. Saouma, Mixed Mode Fracture of Cementitious Bimaterial Interfaces; Part II: Numerical Simulation, *Engineering Fracture Mechanics*, Vol. 60, No. 1, pp. 95-107, May, 1998.

[19] D. Datta, V. Tomar, A. H. Varma, A Path Independent Energy Integral Approach for Analytical Fracture Strength of Steel-concrete Structures with an Account of Interface Effects, *Engineering Fracture Mechanics*, Vol. 204, pp. 246-267, December, 2018.

[20] W. Dong, Z. Wu, X. Zhou, Fracture Mechanisms of Rock-Concrete Interface: Experimental and Numerical, *Journal of Engineering Mechanics*, Vol. 142, No. 7, pp. 1-11, July, 2016.

[21] W. Dong, D. Yang, X. Zhou, G. Kastiukas, B. Zhang, Experimental and Numerical Investigations on Fracture Process Zone of Rock-concrete Interface, *Fatigue & Fracture of Engineering Materials & Structures*, Vol. 40, No. 5, pp. 820-835, May, 2017.

[22] Z. Wang, S. Liu, L. Vallejo, L. Wang, Numerical Analysis of the Causes of Face Slab Cracks in Gongboxia Rockfill Dam, *Engineering Geology*, Vol. 181, pp. 224-232, October, 2014.

[23] P. Lin, W. Zhou, H. Liu, Experimental Study on Cracking, Reinforcement, and Overall Stability of the Xiaowan Super-High Arch Dam, *Rock Mechanics & Rock Engineering*, Vol. 48, No. 2, pp. 819-841, March, 2015.

[24] H. Zhong, H. Li, E. T. Ooi, C. Song, Hydraulic Fracture at the Dam-foundation Interface Using the Scaled Boundary Finite Element Method Coupled with the Cohesive Crack Model, *Engineering Analysis with Boundary Elements*, Vol. 88, pp. 41-53, March, 2018.

[25] Z. Wu, H. Rong, J. Zheng, W. Dong, Numerical Method for Mixed-mode I-II Crack Propagation in Concrete, *Journal of Engineering Mechanics*, Vol. 139, No. 11, pp. 1530-1538, November, 2013.

[26] Z. Yang, X. F. Xu, A Heterogeneous Cohesive Model for Quasi-brittle Materials Considering Spatially Varying Random Fracture Properties, *Computer Methods in Applied Mechanics & Engineering*, Vol. 197, No. 45-48, pp. 4027-4039, August, 2008.

[27] W. Dong, S. Song, B. Zhang, D. Yang, SIF-based Fracture Criterion of Rock-concrete Interface and Its Application to the Prediction of Cracking Paths in Gravity Dam, *Engineering Fracture Mechanics*, Vol. 221, p. 106686, November, 2019.

[28] A. Carpiuc-Prisacari, M. Poncelet, K. Kazymyrenko, F. Hild, H. Leclerc, Comparison Between Experimental and Numerical Results of Mixed-mode Crack Propagation in Concrete: Influence of Boundary Conditions Choice, *Cement & Concrete Research*, Vol. 100, pp. 329-340, October, 2017.

[29] D. Cao, Y. Jiang, J. Wang, B. Ji, O. Alfarraj, A. Tolba, X. Ma, Y. Liu, ARNS: Adaptive Relay-node Selection Method for Message Broadcasting in the Internet of Vehicles, *Sensors (Basel)*, Vol. 20, No. 5, p. 1338, March, 2020.

[30] J. Wang, X. Gu, W. Liu, A. K. Sangaiah, H. Kim, An Empower Hamilton Loop Based Data Collection Algorithm with Mobile Agent for WSNs, *Human-centric Computing & Information Sciences*, Vol. 9, No. 1, pp. 1-14, May, 2019.

[31] D. Cao, B. Zheng, B. Ji, Z. Lei, C. Feng, A Robust Distance-based Relay Selection for Message Dissemination in Vehicular Network, *Wireless Networks*, Vol. 26, No. 3, pp. 1755-1771, April, 2020.

[32] E. B. Tirkolaee, A. A. R. Hosseinabadi, M. Soltani, A. K. Sangaiah, J. Wang, A Hybrid Genetic Algorithm for Multi-trip Green Capacitated Arc Routing Problem in the Scope of Urban Services, *Sustainability*, Vol. 10, No. 5, p. 1366, April, 2018.

[33] J. Wang, Y. Gao, K. Wang, A. K. Sangaiah, S. Lim, An Affinity Propagation-based Self-adaptive Clustering Method for Wireless Sensor Networks, *Sensors (Basel)*, Vol. 19, No. 11, p. 2579, June, 2019.

[34] S. Chu, X. Xue, J. Pan, X. Wu, Optimizing Ontology Alignment in Vector Space, *Journal of Internet Technology*, Vol. 21, No. 1, pp. 15-22, January, 2020.

[35] J. Pan, C. Lee, A. Sghaier, M. Zeghid, J. Xie, Novel Systolization of Subquadratic Space Complexity Multipliers

Based on Toeplitz Matrix-vector Product Approach, *IEEE Transactions on Very Large Scale Integration Systems*, Vol. 27, No. 7, pp. 1614-1622, July, 2019.

[36] S. Hochreiter, J. Schmidhuber, Long Short-term Memory, *Neural Computation*, Vol. 9, No. 8, pp. 1735-1780, November, 1997.

[37] J. Wang, W. Wu, Z. Liao, A. K. Sangaiah, R. S. Sherratt, An Energy-efficient Off-loading Scheme for Low Latency in Collaborative Edge Computing, *IEEE Access*, Vol. 7, pp. 149182-149190, October, 2019.

[38] D. V. Medhane, A. K. Sangaiah, M. S. Hossain, G. Muhammad, J. Wang, Blockchain-enabled Distributed Security Framework for Next Generation IoT: An Edge-cloud and Software Defined Network Integrated Approach, *IEEE Internet of Things Journal*, pp. 1-1, February, 2020.

[39] J. Wang, W. Wu, Z. Liao, R. S. Sherratt, G. Kim, O. Alfarraj, A. Alzubi, A. Tolba, A Probability Preferred Priori Offloading Mechanism in Mobile Edge Computing, *IEEE Access*, Vol. 8, pp. 39758-39767, February, 2020.

[40] T. Wang, L. Qiu, A. K. Sangaiah, A. Liu, Z. A. Bhuiyan, Y. Ma, Edge-computing-based Trustworthy Data Collection Model in the Internet of Things, *IEEE Internet of Things Journal*, Vol. 7, No. 5, pp. 4218-4227, May, 2020.

[41] T. Wang, Y. Liang, Y. Yang, G. Xu, H. Peng, A. Liu, W. Jia, An Intelligent Edge-computing-based Method to Counter Coupling Problems in Cyber-physical Systems, *IEEE Network*, Vol. 34, No. 3, pp. 16-22, May/June, 2020.

[42] K. Cho, B. Van Merrienboer, C. Gulcehre, D. Bahdanau, F. Bougares, H. Schwenk, Y. Bengio, *Learning Phrase Representations Using RNN Encoder-decoder for Statistical Machine Translation*, http://arxiv.org/abs/1406.1078.

[43] M. Schuster, K. K. Paliwal, Bidirectional Recurrent Neural Networks, *IEEE Transactions on Signal Processing*, Vol. 45, No. 11, pp. 2673-2681, November, 1997.

[44] K. Greff, R. K. Srivastava, J. Koutnik, B. R. Steunebrink, J. Schmidhuber, LSTM: A Search Space Odyssey, *IEEE Transactions on Neural Networks and Learning Systems*, Vol. 28, No. 10, pp. 2222-2232, October, 2017.

[45] Z. C. Lipton, J. Berkowitz, C. Elkan, A Critical Review of Recurrent Neural Networks for Sequence Learning, http://arxiv.org/abs/1506.00019.

[46] J. H. Friedman, Greedy Function Approximation: A Gradient Boosting Machine, *Annals of Statistics*, Vol. 29, No. 5, pp. 1189-1232, October, 2001.

Biographies

Jin Wang received the M.S. degrees from Nanjing University of Posts and Telecommunications, China, and Ph.D. degree from Kyung Hee University, South Korea. He is a Professor with Changsha University of Science and Technology. His research interests include wireless sensor networks, and network performance optimization.

Yongsong Zou received the M.S. degree form the Changsha University of Science & Technology, China. He is currently pursuing his Ph.D. degree in School of Hydraulic Engineering, Changsha University of Science & Technology, China. His research interests include underwater wireless sensor networks, wireless sensor networks, machine learning.

Peng Lei received the M.S. and Ph.D.degrees from the Hohai University, China. He is currently a Professor with the Changsha University of Science and Technology, China. His research interests include numerical analysis, health monitoring, and safety assessment of hydraulic structures.

R. Simon Sherratt (Fellow, IEEE) received the M.Sc. and Ph.D. degree from the University of Salford. He is currently a Professor of consumer electronics and the Head of the wireless and computing research. His research topic is on signal processing in consumer electronic devices concentrating on equalization.

Lei Wang received the B.E, M.E and Ph.D. degrees from Changsha University of Science & Technology, China. He is a professor at Changsha University of Science and Technology. His research interests mainly include uncertainty quantification, system reliability of structures, and safe operation risk control of traffic network.